PERGAMON

International Journal of Solids and Structures 37 (2000) 7671–7688

INTERNATIONAL JOURNAL OF SOLIDS and STRUCTURES

www.elsevier.com/locate/ijsolstr

Static analysis of thick rectangular laminated plates: three-dimensional elasticity solutions via differential quadrature element method

F.-L. Liu *

CAD/CAM Laboratory, School of Mechanical and Production Engineering, Nanyang Technological University, Nanyang Avenue, North Spine (N3) Level 2, Singapore 639798

Abstract

This article presents the first endeavor to develop the differential quadrature element method for static solution of three-dimensional elasticity equations of thick rectangular laminated composite plates. The domain decomposition technique is employed to decompose a laminated plate into elements according to material layers. The differential quadrature (DQ) method is then applied to each element where the material properties are continuous to form the element weighting coefficient matrix and element force vector. The discretized element weighting coefficient matrices and element force vectors are assembled together to form the global weighting coefficient matrix and global force vector for the whole plate using connection conditions. The solution for the entire plate is obtained by solving the final algebraic equation system. Detailed formulations and numerical procedures are presented and the convergence characteristics of the method are investigated. The numerical results are then compared, where possible, with the analytical solutions to verify the present solutions. Consequently, some new numerical results are computed and analyzed using the present numerical method for laminated rectangular plates with different boundary conditions, which are not solvable directly by the global DQ method.

Keywords: Three-dimensional elasticity solution; Thick laminated composite plates; Differential quadrature element method; Static analysis; Numerical method

1. Introduction

Three-dimensional elasticity analysis of plate problems has always been attractive for structural mechanics researchers. This is because three-dimensional solutions do not rely on any hypotheses concerning the kinematics of deformation, and do not impose any restrictions on the plate thickness and, therefore, are extremely useful in evaluating the accuracy of the approximate solutions such as various two-dimensional

* Tel.: +65-799-5557/6906; fax: +65-791-1859.
E-mail address: mfllliu@ntu.edu.sg (F.-L. Liu).

0020-7683/00/$ - see front matter
PII: S0020-7683(99)00300-5

plate theories. In addition, the three-dimensional elasticity analysis can provide the physical characteristics, which could not be otherwise predicted by the two-dimensional analysis. In solving the three-dimensional elasticity equations of rectangular plates, quite a number of solution approaches have been proposed. One would find the earlier research work of Pagano (1970), who studied the static bending of infinitely long and finite size composite laminates under sinusoidal lateral loading using an analytical method. The elasticity solutions were compared with the classical thin plate (CTP) theory solutions, and the limitations of the CTP theory were pointed out in his work. Srinivas and Rao (1970) and Srinivas et al. (1970) presented a set of complete analytical analyses on bending, buckling and free vibration of plates with both isotropic and orthotropic materials. Based on the analysis of Srinivas and Rao (1970) and Srinivas et al. (1970), Wittrick (1987) worked out a detailed analytical three-dimensional elasticity solution of simply supported plates for eigenvalue problems of buckling and free vibration and for static deflections under sinusoidal lateral loading. Hutchinson and Zillmer (1983) presented a series of solutions for the free vibration of a free isotropic rectangular plate of finite dimensions. Leissa and Zhang (1983) solved the CFFF isotropic rectangular plate. The notation CFFF denotes a rectangular plate with edge faces: $x=0$, $y=0$, $x=a$ and $y=b$ having clamped (C), free (F), free (F) and free (F) boundary conditions, respectively. Liew et al. (1993, 1994a,b) presented a comprehensive investigation on frequency and mode shapes of SSSS, SCSC, SFSF and CCCC rectangular isotropic plates based on three-dimensional Ritz formulations with orthogonal polynomials. Wang and Tarn (1994) analyzed the bending of simply supported rectangular laminated plates based on an asymptotic solution theory. It is evident that the three-dimensional solutions, available for composite laminated plates with different boundary conditions, reported in the open literature are limited.

Recently, a newly developed numerical method, namely the differential quadrature (DQ) method, has been applied to the elasticity solutions of the three-dimensional isotropic plate problems (Malik and Bert, 1998; Liew and Teo, 1998, 1999; Teo and Liew, 1999). This numerical method was first introduced to the structural analysis field by Bert et al. (1988) and further exploited by Bert et al. (1989) for solving non-linear equations of deflections of orthotropic plates. Since then, much research has been done on both the theoretical development and the engineering applications of the method. An excellent review article contributed by Bert and Malik (1996) has summarized a detailed literature list on both aspects of the DQ method. It has been reported that the DQ method was able to rapidly compute an accurate solution of partial differential equations by using only a few grid points in the respective solution domain and, therefore, has the potential to become an alternative to the conventional numerical methods. However, the further application of the DQ method has been greatly restricted by the drawback that it cannot be directly employed to solve problems with discontinuities. To overcome this drawback, a lot of effort has been made to develop the localized DQ method, namely the quadrature element method (QEM) and the differential quadrature element method (DQEM), by combining the domain decomposition technique with the DQ method for solving a variety class of structural problems having different discontinuities in the geometry, boundary conditions and material properties (Striz et al., 1994, 1997; Chen et al., 1997; Han and Liew, 1996; Liu et al., 1997; Wang and Gu, 1997; Liu and Liew, 1998, 1999a–c; Liu 1999, 2000). The differences between the QEM and the DQEM have been elaborated in previous articles (Wang and Gu, 1997; Liu and Liew, 1999b; Liu, 1999, 2000), and therefore will not be repeated here. Among these analyses, only one- and two-dimensional problems have been treated. No solutions have been reported for solving the three-dimensional plate problems using the localized DQ method. This article represents the first attempt to develop the numerical procedures of the DQEM for the three-dimensional elasticity analysis of laminated composite plates by combining the global DQ method with the domain decomposition method. The detailed formulations for the three-dimensional DQEM analysis for laminated plates and compatibility conditions between elements are derived. The three-dimensional elasticity partial differential equations of the laminated composite plate are not solvable directly by the global DQ method due to the discontinuities in material properties on the interfacial layers. However, they can be solved by the present solution procedures very easily. The detailed numerical procedures are given below.

2. Mathematical formulations

Consider an N_e-layer rectangular laminated composite plate with size $a \times b \times c$ as shown in Fig. 1. Each layer consists of a homogeneous orthotropic material and has a uniform thickness. The properties of the material are given in Table 1. The relative values of the moduli are the same in all the plies, i.e. ($C_{11} : C_{22} : C_{33} : C_{12} : C_{13} : C_{23} : C_{66} : C_{55} : C_{44}$) are identical.

2.1. Equilibrium equations

The laminate can be decomposed into N_e layer elements according to the layer number. For each element, when not considering the body forces, the equations of equilibrium can be written in terms of displacements in Cartesian coordinates as (Srinivas and Rao, 1970)

$$C^{i_e}_{11}\frac{\partial^2 u}{\partial x^2} + C^{i_e}_{66}\frac{\partial^2 u}{\partial y^2} + C^{i_e}_{55}\frac{\partial^2 u}{\partial z^2} + \left(C^{i_e}_{12} + C^{i_e}_{66}\right)\frac{\partial^2 v}{\partial x\,\partial y} + \left(C^{i_e}_{13} + C^{i_e}_{55}\right)\frac{\partial^2 w}{\partial x\,\partial z} = 0, \tag{1a}$$

$$\left(C^{i_e}_{12} + C^{i_e}_{66}\right)\frac{\partial^2 u}{\partial x\,\partial z} + C^{i_e}_{66}\frac{\partial^2 v}{\partial x^2} + C^{i_e}_{22}\frac{\partial^2 v}{\partial y^2} + C^{i_e}_{44}\frac{\partial^2 v}{\partial z^2} + \left(C^{i_e}_{23} + C^{i_e}_{44}\right)\frac{\partial^2 w}{\partial y\,\partial z} = 0, \tag{1b}$$

$$\left(C^{i_e}_{13} + C^{i_e}_{55}\right)\frac{\partial^2 u}{\partial x\,\partial z} + \left(C^{i_e}_{23} + C^{i_e}_{44}\right)\frac{\partial^2 v}{\partial y\,\partial z} + C^{i_e}_{55}\frac{\partial^2 w}{\partial x^2} + C^{i_e}_{44}\frac{\partial^2 w}{\partial y^2} + C^{i_e}_{33}\frac{\partial^2 w}{\partial z^2} = 0, \tag{1c}$$

$$i_e = 1, 2, 3, \ldots, N_e,$$

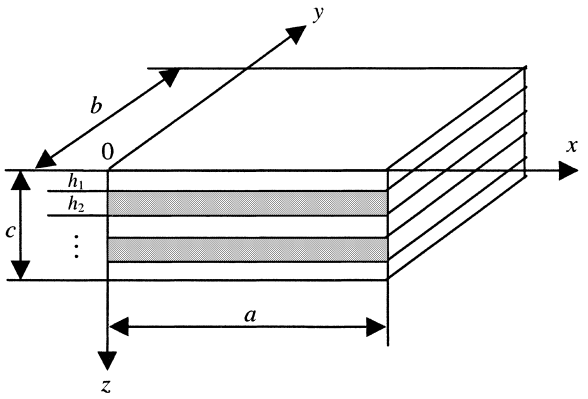

Fig. 1. Configuration of a rectangular thick laminated plate with dimensions $a \times b \times c$.

Table 1
Properties of the orthotropic material in three-ply laminated plate

$C_{22}/C_{11} = 0.543103$
$C_{12}/C_{11} = 0.23319$
$C_{23}/C_{11} = 0.098276$
$C_{55}/C_{11} = 0.159914$
$C_{33}/C_{11} = 0.530172$
$C_{13}/C_{11} = 0.010776$
$C_{66}/C_{11} = 0.262931$
$C_{44}/C_{11} = 0.26681$

where u, v and w are displacements in the x, y and z directions, respectively; $C^{i_e}_{11}$, $C^{i_e}_{22}$, $C^{i_e}_{33}$, $C^{i_e}_{12}$, $C^{i_e}_{13}$, $C^{i_e}_{23}$, $C^{i_e}_{44}$, $C^{i_e}_{55}$ and $C^{i_e}_{66}$ are the nine elastic constants of the orthotropic material of layer i_e.

The constitutive equations for the orthotropic material whose principal axes are parallel to the x, y and z directions of the Cartesian coordinate system can be expressed as

$$\sigma_x = C^{i_e}_{11}\varepsilon_x + C^{i_e}_{12}\varepsilon_y + C^{i_e}_{13}\varepsilon_z, \tag{2a}$$

$$\sigma_y = C^{i_e}_{12}\varepsilon_x + C^{i_e}_{22}\varepsilon_y + C^{i_e}_{23}\varepsilon_z, \tag{2b}$$

$$\sigma_z = C^{i_e}_{13}\varepsilon_x + C^{i_e}_{23}\varepsilon_y + C^{i_e}_{33}\varepsilon_z, \tag{2c}$$

$$\tau_{yz} = C^{i_e}_{44}\gamma_{yz}, \tag{2d}$$

$$\tau_{xz} = C^{i_e}_{55}\gamma_{xz}, \tag{2e}$$

$$\tau_{xy} = C^{i_e}_{66}\gamma_{xy}, \tag{2f}$$

where σ_x, σ_y and σ_z are the normal stresses in the x, y and z directions, and τ_{xy}, τ_{xz} and τ_{yz} are the shear stresses in the x–y, x–z and the y–z planes respectively. ε_x, ε_y and ε_z are the normal strains in the x, y and z directions, and γ_{yz}, γ_{xz} and γ_{xy} are the shear strains in the y–z, x–z and the x–y planes, respectively. For small strains, they can be expressed as follows:

$$\varepsilon_x = \frac{\partial u}{\partial x}, \tag{3a}$$

$$\varepsilon_y = \frac{\partial v}{\partial y}, \tag{3b}$$

$$\varepsilon_z = \frac{\partial w}{\partial z}, \tag{3c}$$

$$\gamma_{yz} = \frac{\partial v}{\partial z} + \frac{\partial w}{\partial y}, \tag{3d}$$

$$\gamma_{xz} = \frac{\partial u}{\partial z} + \frac{\partial w}{\partial x}, \tag{3e}$$

$$\gamma_{xy} = \frac{\partial u}{\partial y} + \frac{\partial v}{\partial x}. \tag{3f}$$

2.2. Boundary conditions

The boundary conditions at the four edge faces of plate where $x = 0, a$ and $y = 0, b$ are defined here as the *edge boundary conditions*, whereas the boundary conditions at the lateral top and bottom surfaces of plate are defined as the *loading conditions* as these are the conditions describing the magnitude of the uniformly distributed pressure load, q.

The edge boundary conditions can be classified into the following three types:

- *Simply supported edge boundary condition* (S)

On $x = 0$ and a: $\sigma_x = 0, \quad v = 0, \quad w = 0,$ (4a–c)

on $y = 0$ and b: $\sigma_y = 0, \quad u = 0, \quad w = 0.$ (5a–c)

- *Clamped edge boundary condition* (C)

$u = 0, \quad v = 0, \quad w = 0.$ (6a–c)

- *Free edge boundary condition* (F)

On $x = 0$ and a: $\sigma_x = 0, \quad \tau_{xy} = 0, \quad \tau_{xz} = 0,$ (7a–c)

on $y = 0$ and b: $\sigma_y = 0, \quad \tau_{xy} = 0, \quad \tau_{yz} = 0.$ (8a–c)

In two-dimensional plate analysis, such as using the classical plate theory or the shear deformation plate theories, it does not matter whether the load is applied on only the top surface of the plate, or on both the top and bottom surfaces of the plate as the deflection of plate is assumed to be independent of the z coordinate. This is not true in the three-dimensional plate analysis. Here one needs to determine whether the load is to be applied to the top surface or both the top and bottom surfaces. This gives rise to the following two general categories of lateral surface loading conditions:

- *Loading on the top surface* (L)

On $z = 0$: $\sigma_z = q, \quad \tau_{xz} = 0, \quad \tau_{yz} = 0,$ (9a–c)

on $z = c$: $\sigma_z = 0, \quad \tau_{xz} = 0, \quad \tau_{yz} = 0.$ (10a–c)

- *Loading on the top and bottom surface* (L')

On $z = 0$: $\sigma_z = q/2, \quad \tau_{xz} = 0, \quad \tau_{yz} = 0,$ (11a–c)

on $z = c$: $\sigma_z = -q/2, \quad \tau_{xz} = 0, \quad \tau_{yz} = 0.$ (12a–c)

3. Method of solution

3.1. Discretizations of equilibrium equations

Suppose that each layer element is further divided into $N_x \times N_y \times N_z$ grid points in the x, y, and z directions, respectively. According to the three-dimensional differential quadrature formulations (Liew and Teo, 1998), the equilibrium Eqs. (1a–c) can be discretized into the following forms:

$$C_{11}^{i_e}\sum_{l=1}^{N_x}A_{il}^{(2)}u_{ljk} + C_{66}^{i_e}\sum_{m=1}^{N_y}B_{jm}^{(2)}u_{imk} + C_{55}^{i_e}\sum_{n=1}^{N_z}C_{kn}^{(2)}u_{ijn} + \left(C_{12}^{i_e} + C_{66}^{i_e}\right)\sum_{l=1}^{N_x}A_{il}^{(1)}\sum_{m=1}^{N_y}B_{jm}^{(1)}v_{lmk} + \left(C_{13}^{i_e} + C_{55}^{i_e}\right)\sum_{l=1}^{N_x}A_{il}^{(1)}\sum_{n=1}^{N_z}C_{kn}^{(1)}w_{ljn} = 0, \tag{13a}$$

$$(C_{12}^{i_e} + C_{66}^{i_e})\sum_{l=1}^{N_x}A_{il}^{(1)}\sum_{m=1}^{N_y}B_{jm}^{(1)}u_{lmk} + C_{66}^{i_e}\sum_{l=1}^{N_x}A_{il}^{(2)}v_{ljk} + C_{22}^{i_e}\sum_{m=1}^{N_y}B_{jm}^{(2)}v_{imk} + C_{44}^{i_e}\sum_{n=1}^{N_Z}C_{kn}^{(2)}v_{ijn} + (C_{23}^{i_e} + C_{44}^{i_e})\sum_{m=1}^{N_y}B_{jm}^{(1)}\sum_{n=1}^{N_z}C_{kn}^{(1)}w_{imn} = 0, \tag{13b}$$

$$\left(C_{13}^{i_e}+C_{55}^{i_e}\right)\sum_{l=1}^{N_x}A_{il}^{(1)}\sum_{n=1}^{N_z}C_{kn}^{(1)}u_{ljn}+\left(C_{23}^{i_e}+C_{44}^{i_e}\right)\sum_{m=1}^{N_y}B_{jm}^{(1)}\sum_{n=1}^{N_z}C_{kn}^{(1)}v_{imn}+C_{55}^{i_e}\sum_{l=1}^{N_x}A_{il}^{(2)}w_{ljk}$$
$$+C_{44}^{i_e}\sum_{m=1}^{N_y}B_{jm}^{(2)}w_{imk}+C_{33}^{i_e}\sum_{n=1}^{N_z}C_{kn}^{(2)}w_{ijn}=0, \tag{13c}$$

$$i_e=1,2,3,\ldots,N_e$$

where $A_{rs}^{(n)}$, $B_{rs}^{(n)}$ and $C_{rs}^{(n)}(r=1,2,3,\ \ldots,Nm;\ s=1,2,3,\ \ldots,Nm;\ m$ can be x, y and z) are the differential quadrature weighting coefficients for the nth-order partial derivatives of u, v and w with respect to the global coordinates x, y and z.

In matrix notation, Eqs. (13a)–(13c) can be rewritten as

$$\mathbf{K}^{\mathrm{e}}\mathbf{d}^{\mathrm{e}}=\mathbf{f}^{\mathrm{e}} \tag{14}$$

in which $\mathbf{K}^{\mathrm{e}}$, $\mathbf{d}^{\mathrm{e}}$ and $\mathbf{f}^{\mathrm{e}}$ are defined as the element weighting coefficient matrix, element displacement vector and element force vector, respectively, and

$$\mathbf{d}^{\mathrm{e}}=\left[u_{1,1,1},v_{1,1,1},w_{1,1,1},u_{1,1,2},v_{1,1,2},w_{1,1,2},\ldots,u_{N_x,N_y,N_z},v_{N_x,N_y,N_z},w_{N_x,N_y,N_z}\right]^{\mathrm{T}}. \tag{15}$$

For the internal nodes of each layer element, $\mathbf{f}^{\mathrm{e}}$ is the null vector and $\mathbf{K}^{\mathrm{e}}$ is determined by Eqs. (13a)–(13c).

Similarly, by substituting Eqs. (3a)–(3f) into Eqs. (2a)–(2f) and discretizing them, one can obtain the stresses as follows:

$$\dot{\sigma}_x=C_{11}^{i_e}\sum_{l=1}^{N_x}A_{il}^{(1)}u_{ljk}+C_{12}^{i_e}\sum_{m=1}^{N_y}B_{jm}^{(1)}v_{imk}+C_{13}^{i_e}\sum_{n=1}^{N_z}C_{kn}^{(1)}w_{ijn}, \tag{16a}$$

$$\sigma_y=C_{12}^{i_e}\sum_{l=1}^{N_x}A_{il}^{(1)}u_{ljk}+C_{22}^{i_e}\sum_{m=1}^{N_y}B_{jm}^{(1)}v_{imk}+C_{23}^{i_e}\sum_{n=1}^{N_z}C_{kn}^{(1)}w_{ijn}, \tag{16b}$$

$$\sigma_z=C_{13}^{i_e}\sum_{l=1}^{N_x}A_{il}^{(1)}u_{ljk}+C_{23}^{i_e}\sum_{m=1}^{N_y}B_{jm}^{(1)}v_{imk}+C_{33}^{i_e}\sum_{n=1}^{N_z}C_{kn}^{(1)}w_{ijn}, \tag{16c}$$

$$\tau_{yz}=C_{44}^{i_e}\left(\sum_{n=1}^{N_z}C_{kn}^{(1)}v_{ijn}+\sum_{m=1}^{N_y}B_{jm}^{(1)}w_{ijn}\right), \tag{16d}$$

$$\tau_{xz}=C_{55}^{i_e}\left(\sum_{n=1}^{N_z}C_{kn}^{(1)}u_{ijn}+\sum_{l=1}^{N_x}A_{il}^{(1)}w_{ljk}\right), \tag{16e}$$

$$\tau_{xy}=C_{66}^{i_e}\left(\sum_{m=1}^{N_y}B_{jm}^{(1)}u_{imk}+\sum_{l=1}^{N_x}A_{il}^{(1)}v_{ljk}\right). \tag{16f}$$

3.2. Discretizations of boundary conditions

The edge boundary conditions (4)–(8) and loading conditions (9)–(12) are discretized into the following forms:

- *Simply supported edge boundary condition* (*S*): For the edge faces $x=0$ and $x=a$,

$$C_{11}^{i_e}\sum_{l=1}^{N_x}A_{il}^{(1)}u_{ljk}+C_{12}^{i_e}\sum_{m=1}^{N_y}B_{jm}^{(1)}v_{imk}+C_{13}^{i_e}\sum_{n=1}^{N_z}C_{kn}^{(1)}w_{ijn}=0, \tag{17a}$$

$$v_{ijk}=0, \tag{17b}$$

$$w_{ijk}=0. \tag{17c}$$

- *Clamped edge boundary condition* (*C*)

$$u_{ijk}=0, \tag{18a}$$

$$v_{ijk}=0, \tag{18b}$$

$$w_{ijk}=0. \tag{18c}$$

- *Free edge boundary condition* (*F*): For the edge faces $x=0$ and $x=a$,

$$C_{11}^{i_e}\sum_{l=1}^{N_x}A_{il}^{(1)}u_{ljk}+C_{12}^{i_e}\sum_{m=1}^{N_y}B_{jm}^{(1)}v_{imk}+C_{13}^{i_e}\sum_{n=1}^{N_z}C_{kn}^{(1)}w_{ijn}=0, \tag{19a}$$

$$\sum_{m=1}^{N_y}B_{jm}^{(1)}u_{imk}+\sum_{l=1}^{N_x}A_{il}^{(1)}v_{ljk}=0, \tag{19b}$$

$$\sum_{n=1}^{N_z}C_{kn}^{(1)}u_{ijn}+\sum_{l=1}^{N_x}A_{il}^{(1)}w_{ljk}=0. \tag{19c}$$

- *Loading condition at the top surface* (*L*) *for* $z=0$

$$C_{13}^{i_e}\sum_{l=1}^{N_x}A_{il}^{(1)}u_{ljk}+C_{23}^{i_e}\sum_{m=1}^{N_y}B_{jm}^{(1)}v_{imk}+C_{33}^{i_e}\sum_{n=1}^{N_z}C_{kn}^{(1)}w_{ijn}=q_{ij}, \tag{20a}$$

$$\sum_{n=1}^{N_z}C_{kn}^{(1)}u_{ijn}+\sum_{l=1}^{N_x}A_{il}^{(1)}w_{ljk}=0, \tag{20b}$$

$$\sum_{n=1}^{N_z}C_{kn}^{(1)}v_{ijn}+\sum_{m=1}^{N_y}B_{jm}^{(1)}w_{imk}=0. \tag{20c}$$

- *Loading condition on the top surface* (*L*) *for* $z=c$

$$C_{13}^{i_e}\sum_{l=1}^{N_x}A_{il}^{(1)}u_{ljk}+C_{23}^{i_e}\sum_{m=1}^{N_y}B_{jm}^{(1)}v_{imk}+C_{33}^{i_e}\sum_{n=1}^{N_z}C_{kn}^{(1)}w_{ijn}=0, \tag{21a}$$

$$\sum_{n=1}^{N_z}C_{kn}^{(1)}u_{ijn}+\sum_{l=1}^{N_x}A_{il}^{(1)}w_{ljk}=0, \tag{21b}$$

$$\sum_{n=1}^{N_z}C_{kn}^{(1)}v_{ijn}+\sum_{m=1}^{N_y}B_{jm}^{(1)}w_{imk}=0. \tag{21c}$$

- *Loading condition on the top and bottom surfaces (L') for $z=0$*

$$C_{13}^{i_e}\sum_{l=1}^{N_x}A_{il}^{(1)}u_{ljk}+C_{23}^{i_e}\sum_{m=1}^{N_y}B_{jm}^{(1)}v_{imk}+C_{33}^{i_e}\sum_{n=1}^{N_z}C_{kn}^{(1)}w_{ijn}=\frac{q_{ij}}{2}, \tag{22a}$$

$$\sum_{n=1}^{N_z}C_{kn}^{(1)}u_{ijn}+\sum_{l=1}^{N_x}A_{il}^{(1)}w_{ljk}=0, \tag{22b}$$

$$\sum_{n=1}^{N_z}C_{kn}^{(1)}v_{ijn}+\sum_{m=1}^{N_y}B_{jm}^{(1)}w_{imk}=0. \tag{22c}$$

- *Loading condition on the top and bottom surfaces (L') for $z=c$*

$$C_{13}^{i_e}\sum_{l=1}^{N_x}A_{il}^{(1)}u_{ljk}+C_{23}^{i_e}\sum_{m=1}^{N_y}B_{jm}^{(1)}v_{imk}+C_{33}^{i_e}\sum_{n=1}^{N_z}C_{kn}^{(1)}w_{ijn}=-\frac{q_{ij}}{2}, \tag{23a}$$

$$\sum_{n=1}^{N_z}C_{kn}^{(1)}u_{ijn}+\sum_{l=1}^{N_x}A_{il}^{(1)}w_{ljk}=0, \tag{23b}$$

$$\sum_{n=1}^{N_z}C_{kn}^{(1)}v_{ijn}+\sum_{m=1}^{N_y}B_{jm}^{(1)}w_{imk}=0. \tag{23c}$$

3.3. Assembly of the differential quadrature layer elements and connection conditions

To obtain the final solution, the element weighting coefficient matrices, the element displacement vectors and the element force vectors should be assembled into a global equation system for all the nodal points of the laminate. To facilitate the assembling procedures, the following rules are used:

- For the internal nodes of each element, the element equilibrium Eqs. (13a)–(13c) are assembled.
- For the boundary nodes on four side faces of plate, the edge boundary conditions (17)–(19) are assembled.
- For the nodes on the top and bottom surfaces of plate, the loading conditions (20)–(23) are assembled.
- For the nodes at the interfacial layers of plate, the connection conditions are used.

The connection conditions for the interfacial nodes should include both the displacement compatibility and the stress compatibility conditions. As the same global nodal number for each conjunction node on the interfacial layers is used, the displacement compatibility conditions are satisfied automatically. Only the stress compatibility conditions are needed. They can be obtained by introducing the equilibrium conditions along plate thickness as follows:

$$(\sigma_z)_{l_e}-(\sigma_z)_{l_e+1}=0, \tag{24a}$$

$$(\tau_{xz})_{l_e}-(\tau_{xz})_{l_e+1}=0, \tag{24b}$$

$$(\tau_{yz})_{l_e}-(\tau_{yz})_{l_e+1}=0, \tag{24c}$$

$$l_e=1,2,\ldots,N_e-1.$$

Thus, the global matrix equation system for the entire laminated plate can be written as

$$\mathbf{Kd}=\mathbf{F}, \tag{25}$$

where **K**, **d** and **F** represent the overall weighting coefficient matrix, global displacement vector and global force vector, respectively. The vector **d** is expressed as

$$\mathbf{d} = [u_1, v_1, w_1, u_2, v_2, w_2, \ldots, u_N, v_N, w_N]^{\mathrm{T}}. \tag{26}$$

Solving the final algebraic equation system by the ordinary linear equation system solver, the solutions to the entire plate can be obtained.

4. Numerical results and discussion

In order to compare the present numerical results with the exact solutions in the open literature, the three-ply laminated plate (0°/90°/0°) analyzed by Srinivas and Rao (1970) is considered. The top and bottom plies are identical with $h_1/c = 0.1$ and $h_2/c = 0.8$. The grid points for each element employed in computations are designated by the following cosine mesh patterns:

$$\Theta(i) = \frac{\alpha}{2}\left(1 - \cos\frac{(i-1)\pi}{N_\alpha - 1}\right), \tag{27}$$

$$i = 1, 2, 3, \ldots, N_\alpha.$$

In Eq. (27), $\Theta(i)$ can either be the $x(i)$, $y(i)$ or $z(i)$ coordinate of the ith point considered and α can be x, y and z.

To examine the validity of the proposed solution procedures, convergence studies are carried out first. The loading condition L is considered. The convergence characteristics of the deflection and stresses at selected locations of the laminated plate with increasing number of the grid points in each layer element are presented for different boundary conditions in Tables 2–4.

Table 2
Convergence of deflections and stresses in simply supported three-ply laminated square plate under a uniform surface load q on the top surface ($z = 0$)[a]

Grid size	$5 \times 5 \times 5$	$7 \times 7 \times 5$	$9 \times 9 \times 5$	$11 \times 11 \times 5$	$11 \times 11 \times 7$	Exact solution[b]
$wC_{11}^2/(cq)$	−156.900	−158.648	−159.439	−159.328	−159.309	−159.38
$(\sigma_x^1)_t/q$	67.4742	64.9974	65.7279	65.2895	65.2748	65.332
$(\sigma_x^1)_b/q$	49.2664	49.0303	48.6863	49.0004	49.0061	48.857
$(\sigma_x^2)_t/q$	4.92657	4.90967	4.87665	4.90772	4.90830	4.9030
$(\sigma_x^2)_b/q$	−4.91018	−4.87460	−4.84871	−4.86591	−4.86532	−4.8600
$(\sigma_x^3)_t/q$	−49.1021	−48.8466	−48.6018	−48.7689	−48.7631	−48.609
$(\sigma_x^3)_b/q$	−67.2165	−64.7783	−65.1533	−65.0780	−65.0689	−65.083
$(\sigma_y^1)_t/q$	47.1082	44.5521	44.8929	44.6473	44.6434	43.566
$(\sigma_y^1)_b/q$	35.3956	33.6793	33.3194	33.5360	33.5389	33.413
$(\sigma_y^2)_t/q$	3.53894	3.42846	3.40508	3.42368	3.42410	3.4995
$(\sigma_y^2)_b/q$	−3.59788	−3.38021	−3.35954	−3.37450	−3.37425	−3.3669
$(\sigma_y^3)_t/q$	−35.9813	−34.7192	−34.6418	−34.7467	−34.7442	−33.756
$(\sigma_y^3)_b/q$	−47.4545	−43.8507	−43.9177	−43.9630	−43.9586	−43.908
$(\tau_{xz})_{ui}/q$	−3.29900	−3.51343	−3.72254	−3.78258	−3.76553	−3.9285
$(\tau_{xz})_m/q$	−3.62353	−3.90401	−4.05594	−4.07543	−4.07177	−4.0959
$(\tau_{xz})_{li}/q$	−3.18372	−3.34061	−3.46163	−3.49465	−3.49443	−3.5154

[a] $c/a = 0.1, h_1/c = 0.1, h_2/c = 0.8, C_{11}^1/C_{11}^2 = 10$, C_{11}^1 and C_{11}^2 are the elastic moduli of the first and second layers of the material in the x direction; $(\sigma_x^{i_e})_t$ and $(\sigma_x^{i_e})_b$, $i_e = 1$, 2 and 3, are the stress values of σ_x at the central point ($x/a = y/b = 0.5$) of the top and bottom surfaces of the i_eth layer material, respectively; $(\sigma_y^{i_e})_t$ and $(\sigma_y^{i_e})_b$, $i_e = 1$, 2 and 3, are the stress values of σ_y at the central point ($x/a = y/b = 0.5$) of the top and bottom surfaces of the i_eth layer material, respectively; and $(\tau_{xz})_{ui}$, $(\tau_{xz})_m$ and $(\tau_{xz})_{li}$ are the transverse shear stresses at the upper interface, the mid-surface and the lower interface of the laminate at $x/a = 0$ and $y/b = 0.5$.

[b] Exact solutions given by Srinivas and Rao (1970).

Table 3
Convergence of deflections and stresses in a three-ply laminated square SCSC plate under a uniform surface load q on the top surface ($z=0$)[a]

Grid size	$5\times5\times5$	$7\times7\times5$	$9\times9\times5$	$11\times11\times5$	$11\times11\times7$
$wC_{11}^2/(cq)$	−106.024	−101.804	−104.275	−103.469	−103.415
$(\sigma_x^1)_t/q$	47.8921	42.2728	43.7427	42.7873	42.7541
$(\sigma_x^1)_b/q$	34.0551	32.3745	31.4471	32.3364	32.3477
$(\sigma_x^2)_t/q$	3.38865	3.23486	3.14811	3.23571	3.23718
$(\sigma_x^2)_b/q$	−3.39123	−3.23976	−3.15583	−3.22973	−3.22987
$(\sigma_x^3)_t/q$	−34.0822	−32.5184	−31.7298	−32.4306	−32.4265
$(\sigma_x^3)_b/q$	−47.8203	−42.1325	−43.1392	−42.5731	−42.5416
$(\sigma_y^1)_t/q$	41.3896	37.1640	38.4688	37.4053	37.4056
$(\sigma_y^1)_b/q$	29.2163	27.6790	24.9288	26.6485	26.6816
$(\sigma_y^2)_t/q$	2.76791	2.74428	2.52386	2.68380	2.69015
$(\sigma_y^2)_b/q$	−2.78880	−2.78282	−2.50467	−2.66140	−2.66548
$(\sigma_y^3)_t/q$	−29.4377	−28.9297	−26.6109	−27.8289	−27.8201
$(\sigma_y^3)_b/q$	−41.3575	−34.2781	−34.4301	−33.5710	−33.5321
$(\tau_{xz})_{ui}/q$	−2.59360	−2.66991	−2.94589	−2.94908	−2.93023
$(\tau_{xz})_m/q$	−2.77728	−2.92628	−3.13197	−3.10158	−3.09600
$(\tau_{xz})_{li}/q$	−2.47722	−2.50128	−2.68118	−2.66246	−2.66033

[a] The notations given here are all the same as those given in Table 2.

Table 4
Convergence of deflections and stresses in a three-ply laminated square CCCC plate under a uniform surface load q on the top surface ($z=0$)[a]

Grid size	$5\times5\times5$	$7\times7\times5$	$9\times9\times5$	$11\times11\times5$	$11\times11\times7$
$wC_{11}^2/(cq)$	−84.6849	−75.6037	−79.8238	−78.1250	−78.0434
$(\sigma_x^1)_t/q$	39.2136	28.8690	33.3172	29.8618	29.72826
$(\sigma_x^1)_b/q$	23.3390	23.6721	19.5976	22.9850	23.0241
$(\sigma_x^2)_t/q$	2.32049	2.36504	1.96118	2.29969	2.30388
$(\sigma_x^2)_b/q$	−2.32539	−2.36085	−1.97546	−2.28166	−2.28414
$(\sigma_x^3)_t/q$	−23.3894	−23.7275	−19.8575	−22.9368	−22.9582
$(\sigma_x^3)_b/q$	−39.1231	−28.8303	−32.7000	−29.7374	−29.6120
$(\sigma_y^1)_t/q$	33.2442	26.5759	28.9047	27.2324	27.1993
$(\sigma_y^1)_b/q$	22.3573	20.2143	17.5925	19.4892	19.5166
$(\sigma_y^2)_t/q$	2.11343	2.00170	1.77218	1.95982	1.96510
$(\sigma_y^2)_b/q$	−2.13451	−2.00696	−1.78946	−1.92392	−1.92626
$(\sigma_y^3)_t/q$	−22.5805	−21.1553	−18.8329	−20.3360	−20.3285
$(\sigma_y^3)_b/q$	−33.2037	−24.3384	−25.6457	−24.2224	−24.1599
$(\tau_{xz})_{ui}/q$	−2.05831	−1.84365	−1.86983	−1.73185	−1.75765
$(\tau_{xz})_m/q$	−1.76017	−1.63401	−1.85550	−2.09861	−2.06440
$(\tau_{xz})_{li}/q$	−1.90009	−1.59648	−1.53955	−1.42634	−1.40849

[a] The notations given here are all the same as those given in Table 2.

It can be seen from these tables that for all the cases considered here, the numerical results of the normalized deflection and stresses at the selected points of the laminated plate converge rapidly with the increase of the number of grid points in each layer element. In Table 2, it is observed that for a simply supported three-ply laminated square plate with $c/a=0.1$ and $C_{11}^1/C_{11}^2=5.0$, the convergent results with maximum deviation error about 2.9% from the exact solutions are obtained when the grid size of each layer element reaches $11\times11\times5$. When the grid size of each layer element becomes $11\times11\times7$, a convergence to four significant figures can be achieved. The numerical results in Tables 3 and 4 show that the convergence rates of the DQEM solutions for SCSC and CCCC boundary conditions are slightly slower than those for

Table 5
Effects of the relative thickness ratio on convergence rates of the deflection and stresses in a simply supported three-ply orthotropic laminate under a uniform load q on the top surface ($z=0$)[a]

c/a	$N_x \times N_y \times N_z$	$wC_{11}^2/(cq)$	e (%)	$(\sigma_x^1)_t/q$	e (%)	$(\sigma_x^1)_b/q$	e (%)	$(\sigma_x^2)_t/q$	e (%)	$(\sigma_y^1)_t/q$	e (%)	$(\sigma_y^1)_b/q$	e (%)	$(\sigma_y^2)_t/q$	e (%)	$(\tau_{xz})_m/q$	e (%)
0.1	$5\times5\times5$	−156.9	1.51	67.4742	3.37	49.2664	0.53	4.92657	0.37	47.1082	5.52	35.3956	5.54	3.53894	3.36	−3.62353	11.0
	$7\times7\times5$	−158.648	0.41	64.9974	0.42	49.0303	0.05	4.90967	0.03	44.5521	0.20	33.6793	0.42	3.42846	0.13	−3.90401	4.12
	$9\times9\times5$	−159.439	0.08	65.7279	0.69	48.6863	0.65	4.87665	0.64	44.8929	0.56	33.3194	0.65	3.40508	0.56	−4.05594	0.39
	$11\times11\times5$	−159.328	0.01	65.2895	0.02	49.0004	0.01	4.90772	0.01	44.6473	0.01	33.536	0.01	3.42368	0.01	−4.07543	0.09
0.2	$5\times5\times5$	−17.0934	0.18	17.0511	8.94	9.11440	5.18	0.91136	5.26	14.2273	7.68	8.98794	0.44	0.89808	1.24	−1.65428	9.04
	$7\times7\times5$	−17.0012	0.72	15.2995	2.25	9.75862	1.52	0.97614	1.47	13.0214	1.45	9.14662	1.32	0.91721	0.86	−1.77815	2.23
	$9\times9\times5$	−17.1464	0.13	16.1389	3.12	9.22109	4.07	0.92288	4.06	13.5237	2.35	8.76164	2.94	0.8832	2.88	−1.81873	0.01
	$11\times11\times5$	−17.1273	0.02	15.6662	0.10	9.61139	0.01	0.96185	0.01	13.2136	0.01	9.02256	0.05	0.90877	0.07	−1.81849	0.01
0.3	$5\times5\times5$	−5.59072	0.32	8.49834	19.0	2.31404	22.2	0.23132	22.0	7.78703	12.6	3.65162	10.1	0.36437	3.53	−0.99436	7.14
	$7\times7\times5$	−5.52443	0.87	6.65983	6.69	3.29362	10.7	0.32827	10.6	6.60148	4.52	4.27092	5.12	0.41711	1.77	−1.05569	1.41
	$9\times9\times5$	−5.57663	0.07	7.50131	5.10	2.65659	10.7	0.26490	10.7	7.16078	3.57	3.82003	5.98	0.37512	2.45	−1.06731	0.33
	$11\times11\times5$	−5.57386	0.02	7.15286	0.22	2.97733	0.07	0.29697	0.07	6.91267	0.02	4.06197	0.03	0.39928	0.03	−1.06873	0.20

[a] $b/a=1.0$, $C_{11}^1/C_{11}^2=5$, $e=|(V-V_c)/V_c|\times100\%$, where V is the instant solution value at a given mesh size, and V_c is the converged value of solution. The other notations given here are all the same as those given in Table 2.

Table 6
Comparison studies for the deflections and stresses in simply supported three-ply laminated square plate under a uniform surface load q on the top surface ($z=0$)[a]

Grid size	$(C_{11})_1/(C_{11})_2=1$		$(C_{11})_1/(C_{11})_2=5$		$(C_{11})_1/(C_{11})_2=10$	
	Present	Exact[b]	Present	Exact[b]	Present	Exact[b]
$wC_{11}^2/(cq)$	−688.628	−688.58	−258.917	−258.97	−159.309	−159.38
$(\sigma_x^1)_t/q$	36.03953	36.021	60.34557	60.353	65.27481	65.332
$(\sigma_x^1)_b/q$	28.53919	28.538	46.69206	46.623	49.00605	48.857
$(\sigma_x^2)_t/q$	28.56844	28.538	9.35157	9.3402	4.9083	4.9030
$(\sigma_x^2)_b/q$	−28.4691	−28.454	−9.29157	−9.2845	−4.86532	−4.8600
$(\sigma_x^3)_t/q$	−28.5195	−28.454	−46.5501	−46.426	−48.7631	−48.609
$(\sigma_x^3)_b/q$	−35.9519	−35.937	−60.163	−60.155	−65.0689	−65.083
$(\sigma_y^1)_t/q$	22.77834	22.210	39.45876	38.491	44.64336	43.566
$(\sigma_y^1)_b/q$	17.69583	17.669	30.17466	30.097	33.53887	33.413
$(\sigma_y^2)_t/q$	17.96263	17.669	6.15493	6.1607	3.4241	3.4995
$(\sigma_y^2)_b/q$	−17.6563	−17.631	−6.06803	−6.0574	−3.37425	−3.3669
$(\sigma_y^3)_t/q$	−17.9162	−17.631	−31.1818	−30.322	−34.7442	−33.756
$(\sigma_y^3)_b/q$	−22.2037	−22.172	−38.7664	−38.715	−43.9586	−43.908
$(\tau_{xz})_{ui}/q$	−2.37889	−2.4029	−3.57683	−3.7194	−3.76553	−3.9285
$(\tau_{xz})_m/q$	−5.36963	−5.3411	−4.35478	−4.3641	−4.07177	−4.0959
$(\tau_{xz})_{li}/q$	−1.99538	−1.9826	−3.24658	−3.2675	−3.49443	−3.5154

[a] $h_1/c=0.1, h_2/c=0.8$, all other notations are the same as those given in Table 2.
[b] Exact solutions given by Srinivas and Rao (1970).

the SSSS boundary conditions. However, all the numerical solutions converged to at least three significant figures at the grid size $11\times11\times7$, for each layer element. To examine the effects of the relative thickness ratio c/a on the convergence of the numerical results, the SSSS laminated plate is analyzed again. The numerical results solved by the present method for different relative thickness ratios are given in Table 5. No significant effects of the relative thickness ratio on the convergence rate have been observed.

To examine the accuracy of the proposed solution methodology, the comparison studies are carried out in Table 6. This comparison is done with the three-dimensional benchmark solutions given by Srinivas and Rao (1970) for the simply supported boundary conditions with different relative thickness ratio and various modular ratios. As seen, the converged DQEM solution shows excellent agreement with the exact solutions. The reliability of present solutions has therefore been confirmed.

Based on the above convergence and comparison studies, the DQEM can now be safely employed to predict the deflection and stress values at any given locations of the laminated plate. To ensure the accuracy of the numerical solutions, the grid size for each layer element is set to $11\times11\times7$. The numerical results computed for a three-ply laminate with SSSS, SCSC and CCCC boundary conditions using the DQEM have been tabulated in Tables 7–9. The effects of the relative thickness ratio c/a and modular ratio C_{11}^1/C_{11}^2 between plies are presented.

It is evident from Tables 7–9 that both the relative thickness ratio c/a and the modular ratio C_{11}^1/C_{11}^2 between plies of laminate bear significant influences on the values of the central deflection and the stresses on plate. In general, the central deflection and all the in-plane and transverse shear stresses decrease markedly as the relative thickness ratio *c/a* increases from 0.1 to 0.3. This is attributed to the effects of shear deformation. As the modular ratio C_{11}^1/C_{11}^2 between the plies of laminate increases, the central deflection decreases greatly. However, the stresses exhibit a different fashion, i.e. the in-plane stresses on the plate, σ_x and σ_y, at the center of the top and bottom surfaces of the plate increases and the transverse shear stress τ_{xz} at the mid-point of side face $x=0$ decreases with the modular ratio C_{11}^1/C_{11}^2, whereas the variations of the in-plane and transverse shear stresses at the interfaces of laminate with the modular ratio C_{11}^1/C_{11}^2 are different for different boundary conditions and different relative thickness ratios. It is also observed that the

Table 7
Deflections and stresses in a simply supported three-ply orthotropic square laminate under a uniform load q on the top surface ($z=0$)[a]

C_{11}^1/C_{11}^2 c/a	1			5			10		
	0.1	0.2	0.3	0.1	0.2	0.3	0.1	0.2	0.3
$wC_{11}^2/(cq)$	−688.6276	−51.81530	−12.99971	−258.9170	−23.71948	−7.01308	−159.3086	−17.12386	−5.57289
$(\sigma_x^1)_t/q$	36.03953	8.92779	3.94599	60.34557	14.62159	6.45823	65.27481	15.65115	7.13714
$(\sigma_x^1)_b/q$	28.53919	6.91078	2.94593	46.69206	10.27669	3.82469	49.00605	9.61235	2.97513
$(\sigma_x^2)_t/q$	28.56844	6.90370	2.93198	9.35157	2.05605	0.76318	4.90830	0.96196	0.29677
$(\sigma_x^2)_b/q$	−28.46912	−6.81877	−2.83087	−9.29157	−1.99391	−0.69223	−4.86532	−0.91753	−0.24855
$(\sigma_x^3)_t/q$	−28.51954	−6.83293	−2.83822	−46.55013	−9.99957	−3.47913	−48.76309	−9.21532	−2.51149
$(\sigma_x^3)_b/q$	−35.95193	−8.88732	−3.89005	−60.16302	−14.49187	−6.24500	−65.06887	−15.49300	−6.85068
$(\sigma_y^1)_t/q$	22.77834	6.10170	2.98814	39.45876	11.07858	5.61872	44.64336	13.21288	6.91413
$(\sigma_y^1)_b/q$	17.69583	4.69987	2.27632	30.17466	8.05820	3.78626	33.53887	9.02730	4.06300
$(\sigma_y^2)_t/q$	17.96263	4.63531	2.14908	6.15493	1.61811	0.74121	3.42410	0.90938	0.39953
$(\sigma_y^2)_b/q$	−17.65634	−4.65228	−2.21870	−6.06803	−1.63677	−0.77786	−3.37425	−0.91756	−0.41792
$(\sigma_y^3)_t/q$	−18.11618	−4.78140	−2.28576	−31.18177	−8.45781	−4.05309	−34.74424	−9.54081	−4.41663
$(\sigma_y^3)_b/q$	−22.20368	−5.94900	−2.90792	−38.76640	−11.08517	−5.74783	−43.95861	−13.29888	−7.13795
$(\tau_{xz})_{ui}/q$	−2.37889	−1.43561	−1.11674	−3.57683	−1.93869	−1.39176	−3.76553	−1.95385	−1.35458
$(\tau_{xz})_m/q$	−5.36963	−2.52007	−1.55338	−4.35478	−1.99456	−1.19689	−4.07177	−1.81870	−1.07082
$(\tau_{xz})_{li}/q$	−1.99538	−0.95720	−0.61345	−3.24658	−1.51795	−0.92177	−3.49443	−1.58423	−0.93474

[a] The notations given here are all the same as those given in Table 2.

Table 8
Deflections and stresses in a SCSC three-ply orthotropic square laminate under a uniform load q on the top surface ($z=0$)[a]

C_{11}^1/C_{11}^2 c/a	1			5			10		
	0.1	0.2	0.3	0.1	0.2	0.3	0.1	0.2	0.3
$wC_{11}^2/(cq)$	−404.715	−33.4378	−9.10915	−160.485	−16.7691	−5.40648	−103.415	−12.8380	−4.52135
$(\sigma_x^1)_t/q$	22.2309	5.80380	2.74646	38.3230	10.3116	5.10641	42.7541	11.9152	6.19387
$(\sigma_x^1)_b/q$	17.5450	4.50140	2.06678	29.6913	7.38355	3.15686	32.3477	7.64451	2.88888
$(\sigma_x^2)_t/q$	17.5576	4.48917	2.05013	5.94211	1.47488	0.62855	3.23718	0.76389	0.28776
$(\sigma_x^2)_b/q$	−17.5521	−4.48369	−2.02598	−5.93641	−1.45618	−0.59830	−3.22987	−0.74711	−0.26569
$(\sigma_x^3)_t/q$	−17.5853	−4.49223	−2.03015	−29.8345	−7.30317	−2.99784	−32.4265	−7.47327	−2.65318
$(\sigma_x^3)_b/q$	−22.0872	−5.80018	−2.74709	−38.1186	−10.313	−5.04646	−42.5416	−11.9153	−6.07993
$(\sigma_y^1)_t/q$	19.3815	5.23351	2.58481	33.3975	9.25480	4.70436	37.4056	10.7759	5.76674
$(\sigma_y^1)_b/q$	14.1693	3.78583	1.82252	24.1931	6.24149	2.73386	26.6816	6.54709	2.55424
$(\sigma_y^2)_t/q$	14.2843	3.67435	1.67070	4.87368	1.23164	0.52108	2.69015	0.64960	0.24514
$(\sigma_y^2)_b/q$	−13.9951	−3.59613	−1.63038	−4.81607	−1.20064	−0.49532	−2.66548	−0.62544	−0.22327
$(\sigma_y^3)_t/q$	−14.2980	−3.67405	−1.66842	−25.4706	−6.20629	−2.53462	−27.8201	−6.27412	−2.19853
$(\sigma_y^3)_b/q$	−17.4335	−4.55338	−2.15298	−30.0920	−8.07748	−3.94744	−33.5321	−9.27107	−4.74965
$(\tau_{xz})_{ui}/q$	−1.92995	−1.21437	−0.97693	−2.81293	−1.58405	−1.19428	−2.93023	−1.60153	−1.17726
$(\tau_{xz})_m/q$	−4.14383	−1.91828	−1.17735	−3.32978	−1.51893	−0.93387	−3.09600	−1.40619	−0.86341
$(\tau_{xz})_{li}/q$	−1.54809	−0.73669	−0.47360	−2.48449	−1.16417	−0.72287	−2.66033	−1.23223	−0.75483

[a] The notations given here are all the same as those given in Table 2.

Table 9
Deflections and stresses in a fully clamped three-ply orthotropic square laminate under a uniform load q on the top surface ($z=0$)[a]

C_{11}^1/C_{11}^2 c/a	1			5			10		
	0.1	0.2	0.3	0.1	0.2	0.3	0.1	0.2	0.3
$wC_{11}^2/(cq)$	−254.9517	−24.95534	−7.53878	−112.39775	−14.04092	−4.84493	−78.04340	−11.28993	−4.14215
$(\sigma_x^1)_t/q$	17.20367	4.21598	1.90807	27.98908	6.89432	3.40748	29.72826	7.82452	4.31574
$(\sigma_x^1)_b/q$	13.65519	3.23332	1.37458	22.11362	4.70859	1.69098	23.02406	4.28467	1.06843
$(\sigma_x^2)_t/q$	13.65633	3.21920	1.35739	4.42444	0.93963	0.33530	2.30388	0.42778	0.10566
$(\sigma_x^2)_b/q$	−13.64625	−3.20081	−1.33269	−4.40450	−0.90856	−0.30700	−2.28414	−0.40404	−0.08784
$(\sigma_x^3)_t/q$	−13.66795	−3.20740	−1.33627	−22.14020	−4.56520	−1.54266	−22.95824	−4.04863	−0.87767
$(\sigma_x^3)_b/q$	−17.12175	−4.23096	−1.93163	−27.87524	−6.93175	−3.40737	−29.61204	−7.85944	−4.26217
$(\sigma_y^1)_t/q$	12.46922	3.84594	2.08740	22.99414	7.41012	4.06091	27.19932	9.05185	5.13404
$(\sigma_y^1)_b/q$	9.10159	2.77581	1.46365	16.72034	4.96072	2.29550	19.51661	5.38695	2.13199
$(\sigma_y^2)_t/q$	9.11199	2.64710	1.30692	3.35974	0.97311	0.43269	1.96510	0.53240	0.20244
$(\sigma_y^2)_b/q$	−8.92614	−2.58459	−1.27212	−3.30164	−0.93821	−0.40704	−1.92626	−0.50497	−0.18132
$(\sigma_y^3)_t/q$	−9.12403	−2.64477	−1.30484	−17.58183	−4.89545	−2.10487	−20.32848	−5.12457	−1.80645
$(\sigma_y^3)_b/q$	−11.09595	−3.28612	−1.69934	−20.54414	−6.38178	−3.35821	−24.15994	−7.68040	−4.16870
$(\tau_{xz})_{ui}/q$	−4.69188	−2.22488	−1.50080	−2.59822	−1.13024	−0.76165	−1.58765	−0.69215	−0.47980
$(\tau_{xz})_m/q$	−4.60119	−2.03305	−1.18328	−2.82265	−1.32480	−0.80018	−2.06440	−1.05058	−0.65275
$(\tau_{xz})_{li}/q$	−4.14295	−1.58024	−0.84791	−2.20437	−0.75751	−0.40029	−1.30849	−0.44629	−0.24082

[a] The notations given here are all the same as those given in Table 2.

in-plane stresses, σ_x and σ_y, at the interfaces of laminate, are discontinuous and the values of the stress differences between two interfacial materials at the same locations on the plate increase as the value of modular ratio C_{11}^1/C_{11}^2 increases. The distributions of the in-plane and transverse shear stresses across the thickness at the center of a cross-ply square laminated plate (0°/90°/0°) with SSSS, SCSC and CCCC boundary conditions are depicted in Figs. 2–4. It is evident that the transverse shear stresses are continuous whereas the values of the in-plane stresses have a sharp jump at the interfaces of laminate.

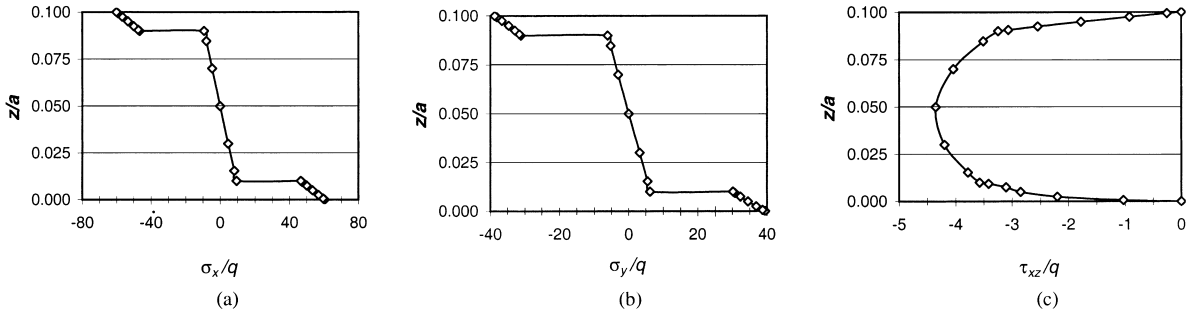

Fig. 2. (a,b) Distributions of in-plane normal stresses σ_x and σ_y across the thickness at the center of a simply supported cross-ply square laminated plate (0°/90°/0°); (c) distribution of transverse shear stress τ_{xz} across the thickness at the middle part of the side face $x=0$.

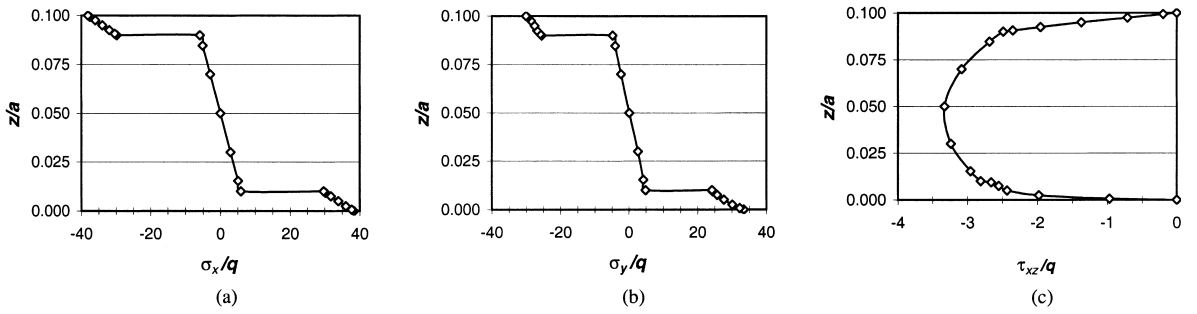

Fig. 3. (a,b) Distributions of in-plane normal stresses σ_x and σ_y across the thickness at the center of a SCSC cross-ply square laminated plate (0°/90°/0°); (c) distribution of transverse shear stress τ_{xz} across the thickness at the middle part of the side face $x=0$.

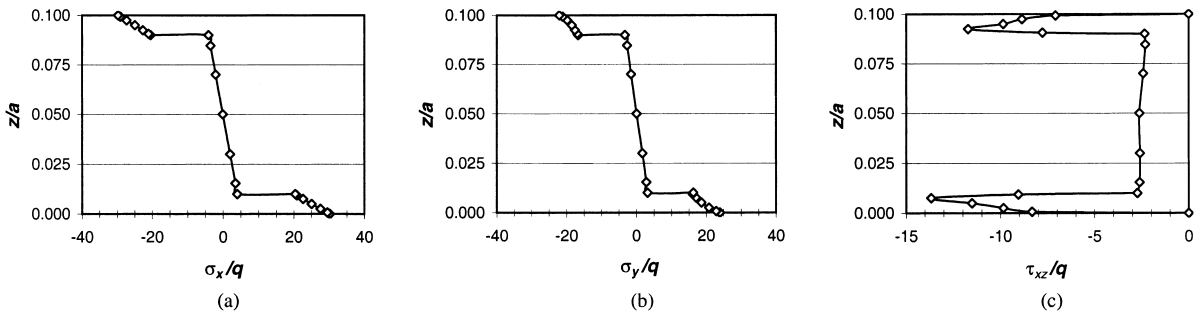

Fig. 4. (a,b) Distributions of in-plane normal stresses σ_x and σ_y across the thickness at the center of a fully clamped cross-ply square laminated plate (0°/90°/0°); (c) distribution of transverse shear stress τ_{xz} across the thickness at the middle part of the side face $x=0$.

5. Conclusion

In this article, the DQEM has been developed for the static analysis of three-dimensional laminated plates by the integration of the domain decomposition technique with the DQ method. The reliability and accuracy of the DQEM have been examined carefully through the convergence and comparison studies for different boundary conditions. The example plates are then analyzed for different boundary conditions, relative thickness ratios and modular ratios between plies of laminate using the developed DQEM, and the detailed results have been presented and analyzed for deflections and stresses at different locations of plates. It is found that the DQEM is capable of yielding accurate numerical results for the composite plates using a relatively coarse mesh.

References

Bert, C.W., Jang, S.K., Striz, A.G., 1988. Two new approximate methods for analyzing free vibration of structural components. AIAA J. 26, 612–618.

Bert, C.W., Jang, S.K., Striz, A.G., 1989. Nonlinear bending analysis of orthotropic rectangular plates by the method of differential quadrature. Comput. Mech. 5, 217–226.

Bert, C.W., Malik, M., 1996. Differential quadrature method in computational mechanics: a review. Appl. Mech. Rev. 49 (1), 1–28.

Chen, W., Striz, A.G., Bert, C.W., 1997. A new approach to the differential quadrature method for fourth-order equations. Int. J. Numer. Meth. Engng. 40 (11), 1941–1956.

Han, J.-B., Liew, K.M., 1996. The differential quadrature element method (DQEM) for axisymmetric bending of thick circular plates. Proc. Int. Conf. Comput. Mech. vol. 3, Techno-Press, Seoul, pp. 2363–2368.

Hutchinson, J.R., Zillmer, S.D., 1983. Vibration of a free rectangular parallelepiped. Trans. ASME, J. Appl. Mech. 50, 123–130.

Leissa, A.W., Zhang, Z.D., 1983. On the three-dimensional vibrations of the cantilevered rectangular parallelepiped. J. Acoust. Soc. America 73, 2013–2021.

Liew, K.M., Hung, K.C., Lim, M.K., 1993. A continuum three-dimensional vibration analysis of thick rectangular plates. Int. J. Solids Struct. 30, 3357–3379.

Liew, K.M., Hung, K.C., Lim, M.K., 1994a. Three-dimensional vibration of rectangular plates: variance of simply supported conditions and influence of in-plane inertia. Int. J. Solids Struct. 31, 3233–3247.

Liew, K.M., Hung, K.C., Lim, M.K., 1994b. Free vibration studies on stress-free three-dimensional elastic solids. Trans. ASME, J. Appl. Mech. 61, 159–165.

Liew, K.M., Teo, T.M., 1998. Modeling via differential quadrature method: three-dimensional solutions for rectangular plates. Comput. Meth. Appl. Mech. Engng. 159, 369–381.

Liew, K.M., Teo, T.M., 1999. Three-dimensional vibration analysis of rectangular plates based on differential quadrature method. J. Sound Vib. 220, 577–599.

Liu, F.-L., 1999. Differential quadrature element method for static analysis of shear deformable cross-ply laminates. Int. J. Numer. Meth. Engng. 46, 1203–1219.

Liu, F.-L., 2000. Rectangular plates on Winkler foundation: differential quadrature element solution. Int. J. Solids Struct. 37, 1743–1763.

Liu, F.-L., Liew, K.M., Han, J.-B., 1997. Development of differential quadrature element method for vibration of Mindlin plates. Proc. Seventh Int. Conf. Computing in Civil & Building Engng. vol. 2, Techno-Press, Seoul, pp. 1151–1156.

Liu, F.-L., Liew, K.M., 1998. Static analysis of Reissner-Mindlin plates by differential quadrature element method. Trans. ASME, J. Appl. Mech. 65, 705–710.

Liu, F.-L., Liew, K.M., 1999a. Vibration analysis of discontinuous Mindlin plates by differential quadrature element method. Trans. ASME, J. Vibr. Acoust. 121, 204–208.

Liu, F.-L., Liew, K.M., 1999b. Differential quadrature element method for static analysis of Reissner-Mindlin polar plates. Int. J. Solids Struct. 36 (33), 5101–5123.

Liu, F.-L., Liew, K.M., 1999c. Differential quadrature element method: a new approach for free vibration analysis of polar Mindlin plates having discontinuities. Comput. Meth. Appl. Mech. Engng. 179 (3–4), 407–423.

Malik, M., Bert, C.W., 1998. Three-dimensional elasticity solutions for free vibration of thick rectangular plates by the differential quadrature method. Int. J. Solids Struct. 35, 299–318.

Pagano, N.J., 1970. Exact solutions for rectangular bidirectional composites and sandwich plates. J. Composite Mat. 5, 20–34.

Srinivas, S., Rao, A.K., 1970. Bending, vibration and buckling of simply supported thick orthotropic rectangular plates and laminates. Int. J. Solids Struct. 6, 1463–1481.

Srinivas, S., Rao, C.V., Rao, A.K., 1970. An exact analysis for vibration of simply supported homogeneous and laminated thick rectangular plates. J. Sound Vibr. 12, 187–199.

Striz, A.G., Chen, W., Bert, C.W., 1994. Static analysis of structures by the quadrature element method (QEM). Int. J. Solids Struct. 31, 2807–2818.

Striz, A.G., Chen, W., Bert, C.W., 1997. Free vibration of high-accuracy plate elements by the quadrature element method. J. Sound Vibr. 202, 689–702.

Teo, T.M., Liew, K.M., 1999. A differential quadrature procedure for three-dimensional buckling analysis of rectangular plates. Int. J. Solids Struct. 36, 1149–1168.

Wang, X., Gu, H., 1997. Static analysis of frame structures by the differential quadrature element method. Int. J. Numer. Meth. Engng. 40, 759–772.

Wang, Y.-M., Tarn, J.-Q., 1994. Three-dimensional analysis of anisotropic inhomogeneous and laminated plates. Int. J. Solids Struct. 31, 497–515.

Wittrick, W.H., 1987. Analytical, three-dimensional elasticity solutions to some plate problems, and some observations on Mindlin's plate theory. Int. J. Solids Struct. 23, 441–464.